



Expression of Perineuronal Nets, Parvalbumin and Protein Tyrosine Phosphatase σ in the Rat Visual Cortex During Development and After BFD

Hui Liu, Haiwei Xu, Tao Yu, Junping Yao, Congjian Zhao & Zheng Qin Yin

To cite this article: Hui Liu, Haiwei Xu, Tao Yu, Junping Yao, Congjian Zhao & Zheng Qin Yin (2013) Expression of Perineuronal Nets, Parvalbumin and Protein Tyrosine Phosphatase σ in the Rat Visual Cortex During Development and After BFD, Current Eye Research, 38:10, 1083-1094, DOI: [10.3109/02713683.2013.803287](https://doi.org/10.3109/02713683.2013.803287)

To link to this article: <https://doi.org/10.3109/02713683.2013.803287>



Published online: 29 May 2013.



Submit your article to this journal 



Article views: 459



View related articles 



Citing articles: 13 View citing articles 

ORIGINAL ARTICLE

Expression of Perineuronal Nets, Parvalbumin and Protein Tyrosine Phosphatase σ in the Rat Visual Cortex During Development and After BFD

Hui Liu^{1,2}, Haiwei Xu^{1,2}, Tao Yu^{1,2}, Junping Yao^{1,2}, Congjian Zhao^{1,2} and Zheng Qin Yin^{1,2}

¹Southwest Eye Hospital, Southwest Hospital, Third Military Medical University, Chongqing, China and

²Key Lab of Visual Damage and Regeneration & Restoration of Chongqing, Chongqing 400038, China

ABSTRACT

Purpose of the Study: Protein tyrosine phosphatase σ (PTP σ) acts as a neuronal receptor for chondroitin sulfate proteoglycans (CSPGs). CSPGs have inhibitory effects on experience-dependent plasticity and usually form lattice-like cell coatings that surround the parvalbumin (PV) interneurons in the visual cortex (VC). We investigated developmental changes and the effect of binocular form deprivation (BFD) on PTP σ , perineuronal nets (PNNS) and their tempo-spatial relationships with PV neurons in the VC.

Materials and Methods: Double-immunostaining was used to observe the coexpression pattern of PNNS staining by biotinylated wisteria floribunda lectin (WFA) with PV neurons. The expression of PTP σ in the VC of Long Evans rats was detected by real-time quantitative PCR, immunohistochemistry and western blots. The changes in the number of PV/WFA/PTP σ labeled cells in layer IV of the VC and its proportion of PV neurons were examined during development and after BFD.

Results: The expression of PV neurons wrapped by PNNS was increased, particularly in the first half of the critical period, and the ratio for PV neurons reached the highest level (over 75%) at adulthood, indicating that PNNS may play an important role in the maturation of PV neurons during the critical period. BFD decreased the density of PNNS and the percentage of PV neurons with PNNS. This result suggests that the number of PNNS surrounding PV neurons may be experience-dependent. Meanwhile, the CSPG receptor PTP σ was maintained at its lowest level during the critical period and could be modulated by BFD after the critical period. The percentage of PV/WFA/PTP σ -positive cells in PV population increased during development and reached its highest ratio at adulthood, which could also be reversed by BFD.

Conclusions: The changes in the coexpression of PNNS, PV and PTP σ provide valuable insights into the connection between CSPGs and PV neurons.

Keywords: Chondroitin sulfate proteoglycan, development, protein tyrosine phosphatase, rats, visual cortex

INTRODUCTION

Chondroitin sulfate proteoglycans (CSPGs) are key components of the central nervous system extracellular matrix. They are comprised of a core protein and chondroitin-sulfate glycosaminoglycan chains,¹ which

condense at high concentrations into lattice-like perineuronal nets (PNNS). The degradation of chondroitin-sulfate chains with chondroitinase ABC reactivates ocular dominance plasticity in adult rats like the effect of dark exposure and binocular form deprivation (BFD) which could induces ocular dominance

Received 14 August 2012; revised 24 April 2013; accepted 3 May 2013; published online 29 May 2013

Correspondence: Zheng Qin Yin, M.D., Ph.D., Southwest Eye Hospital, Southwest Hospital, Third Military Medical University, Chongqing, 400038, People's Republic of China. Tel: 86-23-68754401. Fax: 86-23-65460711. E-mail: qinzyin@yahoo.com.cn
Haiwei Xu, PhD, Southwest Eye Hospital, Southwest Hospital, Third Military Medical University, Chongqing, 400038, People's Republic of China. E-mail: haiweixu2001@163.com

shift during the adulthood,^{2–4} suggesting that CSPG-enriched PNNs exert powerful inhibitory control on the ocular dominance plasticity. However, the underlying mechanism by which the degradation of chondroitin-sulfate-GAG chains results in the restoration of plasticity remains largely enigmatic.

The inhibition of visual cortex (VC) plasticity is also thought to be determined by the maturation of parvalbumin (PV)-positive neurons.^{5,6} PV interneurons function as essential mediators of feed-forward inhibition, network synchrony and oscillations, and the timing of the critical period.⁷ Interestingly, it has been shown that PNNs completely ensheathe some cortical neurons, especially PV neurons.³ However, the effect of PNNs on PV neurons has not yet been determined.

A recent study has demonstrated that the neuronal protein tyrosine phosphatase σ (PTP σ) acts as a receptor for CSPGs.⁸ This finding provides important mechanistic clues about CSPG function. PTP σ belongs to the vertebrate family of type-II a receptor protein tyrosine phosphatases (RPTPs). RPTPs comprise a large and divergent molecular family that controls the extent of phosphorylation of the tyrosine residues that transduce signals from the extracellular environment to the cytoplasm.⁹ In particular, the type-II a RPTP subfamily plays an important role in axon guidance, synapse formation and growth cone function.^{10,11} Members of this subfamily have been reported to be involved in *Xenopus* and chicken visual system development by controlling retinal ganglion cell axon extension rates.^{12,13}

PTP σ is composed of two cytoplasmic phosphatase domains and multiple extracellular immunoglobulin domains followed by fibronectin type III (FNIII)-like repeats.¹⁴ PTP σ binds to neural CSPGs with high affinity. This binding involves a specific site on the first immunoglobulin-like domain of PTP σ and the chondroitin-sulfate-chains of the CSPG.¹⁵ It is abundantly expressed in both the developing and mature mammalian nervous systems,¹⁶ acting to inhibit axon growth and slow axon regeneration.^{14,17}

However, the temporospatial distribution pattern of PTP σ and its coexpression with PNNs and PV neurons in the VC during development and after BFD in adult animals has not yet been characterized. As PNN envelopes can be detected using N-acetylgalactosamine-specific lectins such as *Wisteria floribunda* lectin (WFA), we refer to structures that have been labeled using WFA as PNNs in this study.

Using Q-PCR, immunohistochemistry, co-immunostaining and western blots, we examined the developmental changes and the effect of BFD on the density of neurons double-stained for WFA and PV (WFA/PV cells), PTP σ and changes in the number of WFA/PV neurons coexpressing PTP σ (PV/WFA/PTP σ cells) in the VC of Long Evans rats.

MATERIALS AND METHODS

Animals and Binocular Form Deprivation

Long Evans rats of either sex were divided into five groups: PW1 (6–8 days, before eye opening), PW3 (20–22 days, beginning of the critical period), PW5 (34–36 days, middle to later stage of the critical period), PW7 (48–50 days, end of the critical period) and PW9 (62–64 days, adult).¹⁸

According to our previous protocol, with some modification,¹⁹ binocular form deprivation was initiated at postnatal days 48–50 (the end of the critical period) and continued for 14 days, and the euthanization and analysis were performed at PW9. The eyelid margins of both eyes were trimmed and sutured under urethane anesthesia (1.6 g kg⁻¹, i.p.; 20% solution in saline; Sigma-Aldrich, Saint Louis, MO). The BFD group was inspected twice a day for holes in the sutured eyelids. We immediately repaired the holes, if necessary. After 14 days, rats whose eyelid fusion had a hole or those with any indications of corneal damage or cataract were removed from the study. The BFD and normal rats were treated in accordance with principles of laboratory animal care and the ARVO Statement for the Use of Animals in Ophthalmic and Vision Research; ethical approval was obtained from the Third Military Medical University. Rats were housed in a specific pathogen-free animal room under a 12 h light/12 h dark cycle and provided with food and water *ad libitum*.

Real-time Quantitative PCR (Q-PCR) analysis

The primary VCs (lateral 2–4 mm, posterior 0–2 mm; $n=9$ for each group) were dissected (over ice) away from the underlying white matter and immediately frozen in liquid nitrogen for subsequent real-time PCR analysis. The tissue from each animal was used for a single RNA preparation. Nine individual samples were tested. In brief, RNA was isolated with Trizol (Invitrogen, Carlsbad, CA), according to the manufacturer's instructions. Contaminating DNAs were removed using the TURBO DNA-freeTM Kit (Ambion, Austin, TX), and cDNAs were synthesized from 2 μ g of total RNA with the PrimeScriptRT reagent Kit (TAKARA, Shiga, Japan). Real-time PCR was carried out in a Bio-Rad 5-Color System (Bio-Rad, Hercules, CA) using SYBR Green master mix (QIAGEN). Primers were designed online with IDT SciTools and used spanned introns. The sequences and product sizes are reported in Table 1. To confirm the specificity of PCR products, melting curves were determined using iCycler software, and samples were run on an agarose gel. Reactions were performed in triplicate for each sample. The cycling parameters

TABLE 1 Real-time PCR primer sequences and product sizes.

Genes(rat)	Sequence	Product size (bp)
PTP σ	Up-5'-GCCGCCGATAGCCGTCCACATAG-3' Down-5'-CCGCCCATTCCCACAGAC-3'	262
GAPDH	Up-5'-ACCCATCACCATCTTCCAGGAG-3' Down-5'-GAAGGGCGGAGATGATGAC-3'	159

were as follows: 1 cycle at 94 °C for 5 min, 35 cycles at 94 °C for 30 s, 57 °C for 30 s, 72 °C for 30 s, 1 cycle at 72 °C for 10 min, 4 °C ∞. Q-PCR fluorescence measurements were taken after every cycle, and the cycle threshold (CT) was recorded for each reaction. The expression level of PTP σ mRNA was measured using the $2^{-\Delta\Delta Ct}$ method and normalized to GAPDH levels. Significance was evaluated by one-way ANOVA followed by a least significant difference multiple-comparison *t*-test.

Western Blots

The primary VCs ($n=9$ for each group) were isolated and rinsed in 0.01 PBS, drained, and homogenized in ice-cold RIPA Lysis buffer (Beyotime, Shanghai, China). The lysates were cleared by centrifugation at 15,000 g for 5 min at 4 °C. Protein concentration was determined using the BCA Protein Assay (Beyotime, Shanghai, China) according to the manufacturer's instructions. Total-protein samples (50 μ g per lane) were separated on a 10% SDS-polyacrylamide gel and then transferred onto PVDF membranes. The PVDF membranes were blocked in 5% non-fat milk in Tris-buffered saline with 0.1% Tween-20 (TBST) at room temperature for 1 h. The blots were incubated in rabbit anti-PTP σ antibody (1:400; ProteinTech, 13008-1-AP, Chicago, IL) and mouse anti-GAPDH antibody (1:1000; ProteinTech, 60004-1-Ig) at 4 °C overnight. The membranes were washed with TBST and further incubated in secondary antibodies. Immunoreactive bands were visualized using chemiluminescence development (SuperSignal West Pico Chemiluminescent Substrate; Pierce, Rockford, IL). Labworks 4.6 was used to analyze the gray scale of these blots.

Immunohistochemistry

Animals ($n=9$ for each group) were euthanized with urethane and then transcardially perfused with normal saline followed by 4% paraformaldehyde in 0.1 M phosphate buffer. Brains were removed and post-fixed in 4% paraformaldehyde overnight at 4 °C; they were then cryoprotected in PBS containing 30% sucrose for at least 24 h at 4 °C. A series of coronal sections for histological staining, extending approximately 1–3 mm from the occipital poles and including the VCs, were cut at 30 μ m using a freezing microtome.

Immunohistochemistry was performed as described previously.²⁰ VC sections were rinsed with PBS and then incubated in a blocking solution composed of 5% normal goat serum and 0.3% Triton X-100 (Sigma-Aldrich, Saint Louis, MO) in PBS for 1 h. Sections were then incubated overnight at 4 °C in a solution of 2% normal goat serum and 0.3% Triton X-100 containing a PTP σ antibody (1:100; ProteinTech). After a thorough rinse, the sections were incubated with a Cy3-labeled goat anti-rabbit IgG (1:500; Beyotime, A0516, Shanghai, China) for 2 h at room temperature. Finally, the cell nuclei were labeled using 4,6-diamidino-2-phenylindole (DAPI; Beyotime, C1002, Shanghai, China).

Sections were also double-labeled after incubation with PV (monoclonal mouse PV, 1:1000; Abcam, ab64555, Cambridge, UK) and biotinylated WFA (1:200; Vector, B-1355, Burlingame, CA) overnight at 4 °C. The sections were thoroughly washed and were then incubated with FITC-labeled goat anti-mouse (1:100; Zhongshan Goldenbridge, ZF-0312, Beijing, China) and AMCA-conjugated streptavidin (1:200; Vector, SA-5008, Burlingame, CA) for 2 h at room temperature. For triple fluorescent labeling, the sections were incubated with a cocktail composed of WFA and antibodies for PTP σ and PV, with the same concentrations noted above. After three rinses with PBS, the sections were processed for 2 h with a second cocktail of Cy3-labeled goat anti-rabbit IgG (1:500; Beyotime, Shanghai, China), FITC-labeled goat anti-mouse IgG (1:100; Zhongshan Goldenbridge, Beijing, China) and AMCA-conjugated streptavidin (1:200; Vector, Burlingame, CA). Bovine serum albumin or normal rabbit serum replaced primary antibodies in negative controls. Control sections in which primary antibodies or secondary antibodies were omitted showed no labeled cells. Besides, testing the PTP σ antibody on dorsal root ganglion as the positive control tissue according to previous reports were also done (see supplemental data).⁸

Quantitative Analysis of Immunohistochemistry

The VC layers were defined using previously reported methods.^{3,18} Fields from VC sections were acquired from layer II-III, layer IV and deep layer V-VI. Analyses were performed on five sections from each of the nine animals in each group (PW1, PW3, PW5, PW7, PW9 and BFD), according to the method

described by Tropea.²¹ To visualize the labeled cells across the full thickness (all layers) of the cortex, the slides were inspected using a laser-scanning confocal microscope (Leica TCS 4D; laser lines at 488, 543, 633 nm, Leica, Wetzlar, Germany) at lower power magnification (10 \times). The quantification of each layer was performed at high-power magnification (63 \times), with confocal images collected in z-stacks. The colocalization of two or more markers was established when the respective fluorescence signal was clearly present at the same range within the Z-axis for each marker, and it was confirmed by a color change of overlapping markers. The numerical aperture of the 63 \times lens is 1.4, and the z-step size was 1.43 μ m. Image Pro Plus 4.5 was used to quantify the density of PTP σ -, PV-, and WFA-positive cells within 10 sample boxes (each box = 625 μ m 2) randomly chosen in each layer. To quantify the changes during development and to compare different situations, a masked morphometric study was performed, in which the individual who measured the sections did not know the features of each case (neither the age of the rats nor whether they belonged to the BFD group). Double- and triple-labeled cells were also counted.

The non-parametric Kruskal-Wallis test was used to evaluate age-dependent differences in all groups, followed by the Mann-Whitney *U* test to determine significant differences between specific groups. A level of $p \leq 0.05$ was considered to be statistically significant. All statistics were carried out using SPSS software (Ver. 11.5, IBM, Rochester, MN).

RESULTS

Developmental Changes and Effects of BFD on the PNN/PV Coexpression in the VC

WFA (PNNs) staining was not detected at PW1. Staining of the somata, short lengths of the proximal dendrites, and the extracellular space was observed at PW3 (Figure 1). Dendritic labeling becomes more apparent with increasing age of the cortex (see also Figure 5). During the first half of the VC critical period, between PW3–5, the density of WFA staining increased significantly in layers II–III and layer IV ($p < 0.01$, PW3 versus PW5) (Figure 2A and C). A significant increase in WFA-labeled cells was also observed in both layers after the end of the critical period ($p < 0.05$, PW7 versus PW9 in layers II–III; $p < 0.01$, PW7 versus PW9 in layer IV). However, BFD significantly decreased the number of WFA-positive cells in both layers ($p < 0.01$, BFD versus PW7/PW9) (Figure 2A, 2C).

PV-positive cells were present in the VC by PW3 (Figure 1). The number of PV-labeled neurons was highest at PW3 ($p < 0.01$, PW3 versus PW5), and it then decreased with age in both layers until PW7

($p < 0.01$, PW5 versus PW7) and stayed at the adult level between PW7–9 ($p > 0.05$, PW7 versus PW9) in layers II–III and layer IV (Figure 2A, 2C). However, the density of WFA/PV positive cells increased significantly between PW3–5 in both layers, closely paralleling the change observed for WFA-positive cell numbers ($p < 0.01$, PW3 versus PW5) (Figure 2A, 2C). In layers II–III, the number of WFA/PV positive cells stayed at a relatively stable level after PW5 ($p > 0.05$, PW5 versus PW7/PW9) (Figure 2A). In layer IV, the density of double-labeled cells was highest at PW5 ($p < 0.01$, PW5 versus PW7; $p < 0.05$, PW5 versus PW9), followed by a decrease at PW7; the density then increased with the same trend as the increase of WFA-positive cell numbers at PW9 ($p < 0.01$, PW7 versus PW9) (Figure 2C). Although BFD did not change the number of PV neurons, the density of WFA/PV positive cells was reduced after BFD ($p < 0.01$, BFD versus PW9 in layers II–III and layer IV; $p < 0.01$, BFD versus PW7 in layers II–III; $p < 0.05$, BFD versus PW7 in layer IV) (Figures 2A and C).

Next, we analyzed the percentages of WFA- and PV-positive cells that were double-labeled for WFA and PV. In layers II–III and layer IV, although the number of WFA-positive cells increased with age, the ratio of WFA/PV positive cells to WFA-positive cells decreased after PW3 ($p < 0.01$, PW3 versus PW5) and remained at its lowest level between PW7–9 ($p < 0.01$, PW5 versus PW7 in layer IV; $p < 0.05$, PW5 versus PW7 in layers II–III; $p > 0.05$, PW7 versus PW9) (Figure 2B, 2D). However, although the density of PV neurons decreased with age, the percentage of PV neurons double-labeled for WFA and PV showed an opposite trend (Figure 2B, 2D). In layers II–III, the ratio of WFA/PV positive cells to PV neurons increased until PW7 ($p < 0.01$, PW3 versus PW5; $p < 0.01$, PW5 versus PW7) and stayed at the adult level between PW7–9 ($p > 0.05$, PW7 versus PW9) (Figure 2B). In layer IV, the percentage of WFA/PV double-labeled PV neurons increased at PW5 ($p < 0.01$, PW5 versus PW3), followed by a decrease at PW7 ($p < 0.05$, PW5 versus PW7); the percentage then returned to the PW5 level at PW9 ($p < 0.01$, PW7 versus PW9; $p > 0.05$, PW5 versus PW9) (Figure 2D). The ratio of WFA/PV positive cells to WFA-positive cells did not change after BFD. However, the percentage of WFA/PV double-labeled PV neurons was reduced after BFD ($p < 0.01$, BFD versus PW7/PW9) (Figure 2B, 2D), most likely due to the decreased number of WFA/PV positive neurons after BFD in layers II–III and layer IV.

Expression of PTP σ in the VC During Postnatal Development and After BFD

RNA was isolated from the VC of PW1, PW3, PW5, PW7, PW9 and BFD rats. PCR primers for GAPDH

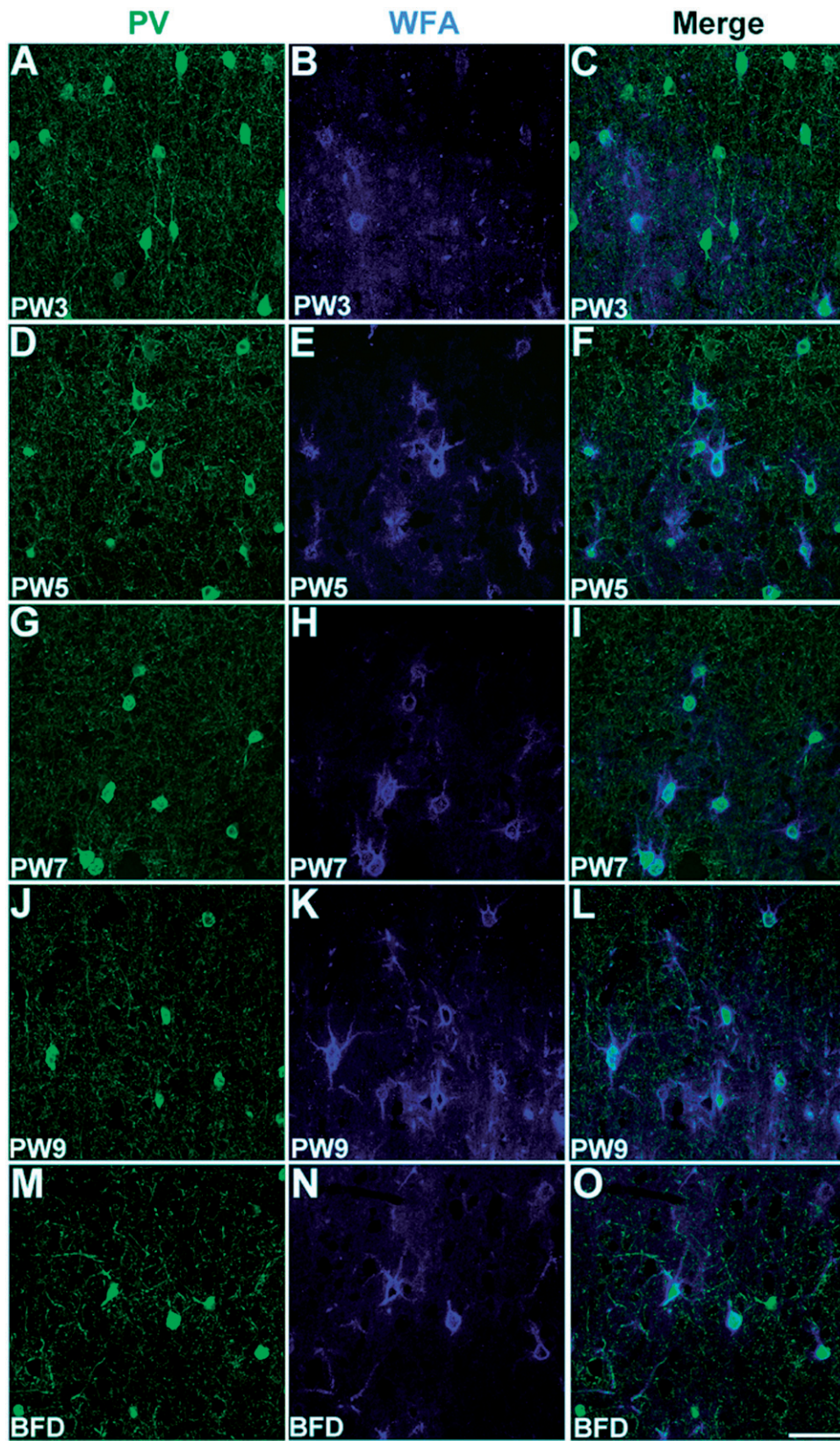


FIGURE 1 Parvalbumin neurons (green) wrapped by PNNs (blue) in layer IV of the rat primary visual cortex from each group. PW3 (A–C), PW5 (D–F), PW7 (G–I), PW9 (J–L), BFD (M–O). Scale bar = 50 μ m.

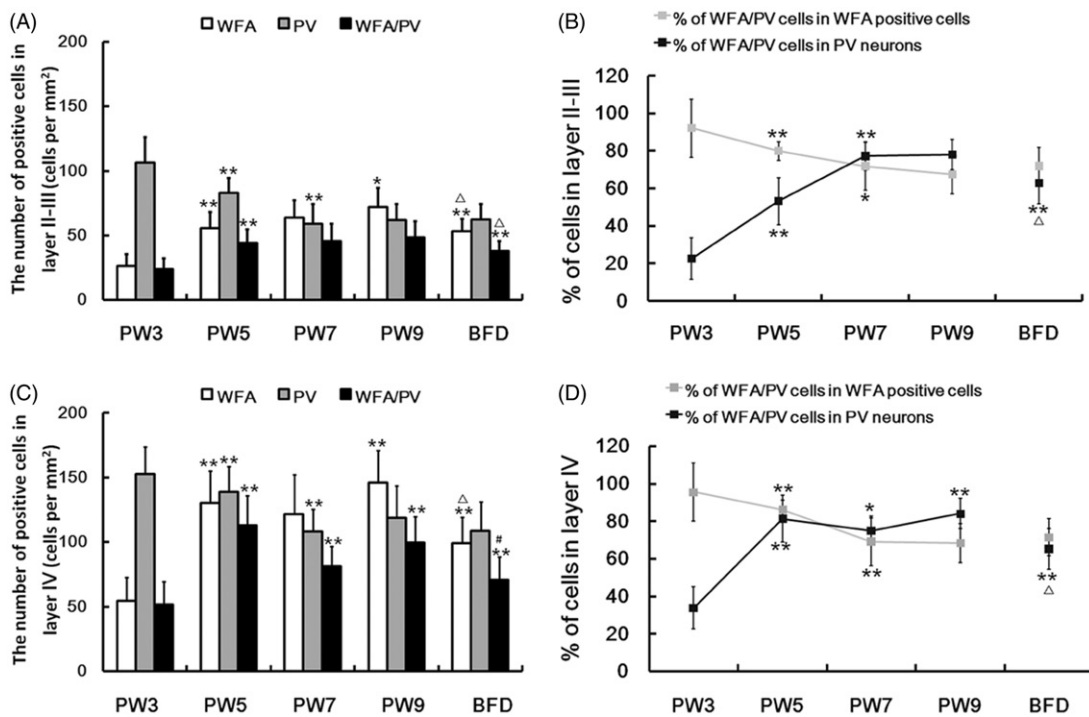


FIGURE 2 Quantitative analysis of WFA, PV and WFA/PV double-labeled neurons in layer II-III (A–B) and layer IV (C–D) of the rat primary visual cortex from different groups. Values are expressed as the mean \pm S.E.M., $n=9$ animals per age. Mann–Whitney U -test was used to assess the statistical significance of the group differences. (A): ** $p<0.01$, * $p<0.05$ in relation to the immediately preceding stage; $\Delta p<0.01$, BFD versus PW7. (B): ** $p<0.01$, * $p<0.05$ in relation to the immediately preceding stage; $\Delta p<0.01$, BFD versus PW7. (C): ** $p<0.01$ in relation to the immediately preceding stage; $\Delta p<0.01$, # $p<0.05$, BFD versus PW7. (D): ** $p<0.01$, * $p<0.05$ in relation to the immediately preceding stage; $\Delta p<0.01$, BFD versus PW7.

and PTP σ (*Ptprs*) were designed and tested in Q-PCR reactions. PTP σ mRNA was already present within the VC by PW1 at a level that was significantly higher ($p<0.01$) than observed at subsequent ages and in the BFD group (Figure 3N). PTP σ levels declined during the first half of the VC critical period and ranged between PW3 and PW5 ($p<0.01$, PW3 versus PW5). The adult levels of PTP σ at PW9 were higher than those observed at the end of the critical period ($p<0.01$, PW7 versus PW9) but were not significantly different from those at the start of the critical period (PW3) ($p>0.05$, PW3 versus PW9) (Figure 3N). However, BFD decreased PTP σ mRNA expression after the critical period ($p<0.01$, BFD versus PW7/PW9) (Figure 3N).

Cellular PTP σ was expressed in all layers of the VC throughout development. PTP σ immunolabeling appeared to be mainly localized within the cytoplasm and apical or primary dendrites (Figure 3A–3L). Most of the PTP σ -positive cells (92.2 \pm 2.1%, $n=3$ rats) at PW9 were shown to be neurons by double staining with antibodies to the neuronal marker MAP-2 (Supplementary Data, Figure S1). The changes in PTP σ -positive cell numbers closely followed the trends observed in the PCR analysis: within the individual VC layers, PTP σ -positive cell numbers were highest at PW1 ($p<0.01$, PW1 versus PW3) and lowest during the critical period ($p<0.01$, PW3 versus

PW5/PW7) (Figure 3M). Cell numbers had again significantly increased by PW9 ($p<0.01$, PW7 versus PW9) but were not significantly different from those at the start of the critical period (PW3) in all layers (Figure 3M). BFD could also decrease the densities of PTP σ positive cells in all layers in the VC ($p<0.01$, BFD versus PW9), but only in layers II–III and layer IV did the PTP σ -positive cell numbers decrease when compared with PW7 ($p<0.01$, BFD versus PW7). PTP σ -positive cell numbers were higher in layers V–VI compared to other layers ($p<0.01$) from PW3 to PW9 but were not significantly different from layers II–III at PW1. Layers II–III significantly differed from layer IV only at PW1 ($p<0.01$). However, BFD could not change the distribution pattern of PTP σ -positive cells between layers in the VC ($p<0.01$, layers V–VI versus layers II–III/layer IV) (Figure 3M).

To establish whether changes in the PTP σ mRNA level and the distribution of PTP σ -immunostained cells in the VC during development correspond to different protein levels, tissue from the primary visual area was extracted, homogenized and run on western blots. The total protein content from brain extracts was normalized to GAPDH (Figure 4A). Similar to the data presented for PCR and immunohistochemistry, the PTP σ protein expression was highest at PW1 ($p<0.01$) and decreased significantly during the first half of the critical period, reaching its lowest point at

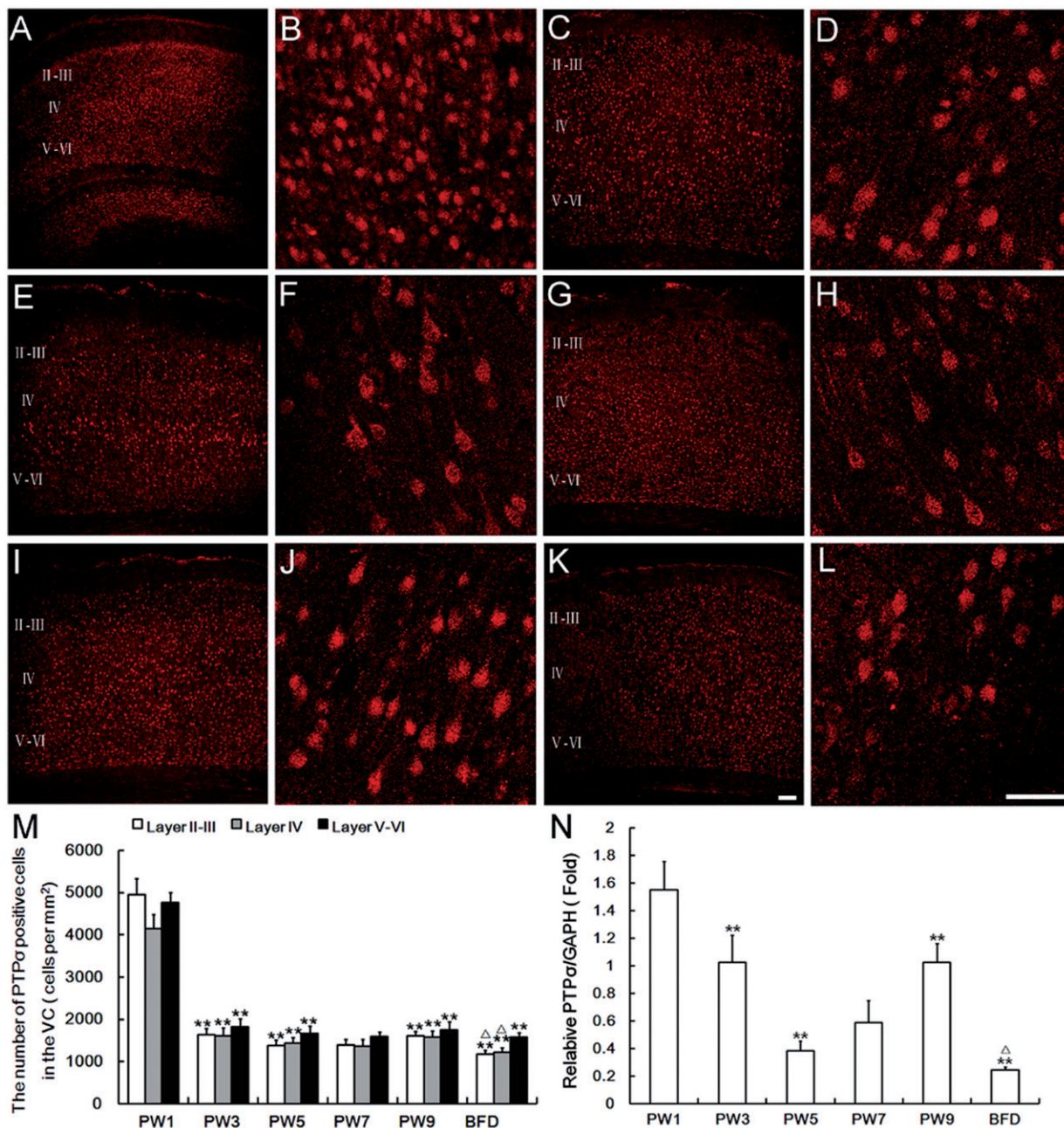


FIGURE 3 Q-PCR analysis and immunoreactivity of PTP σ in the visual cortex of the Long Evans rats. (A), (C), (E), (G), (I), (K): Low-magnification photomicrographs show PTP σ -positive cells in the visual cortices of rats aged PW1 (A), PW3 (C), PW5 (E), PW7 (G), PW9 (I) and BFD (K). Photomicrographs were taken in the transitional region between the monocular and binocular visual cortices. (B), (D), (F), (H), (J), (L): Higher-magnification photomicrographs show PTP σ staining in layer IV at the same age. Scale bars = 50 μ m. (M): Values are expressed as the mean \pm S.E.M., $n=9$ animals per group. Mann–Whitney U -test was used to assess the statistical significance of the group differences (** $p<0.01$ in relation to the immediately preceding stage; $\Delta p<0.01$, BFD versus PW7). (N): Q-PCR analysis of relative PTP σ to GAPDH (Fold). Values are expressed as the mean \pm S.E.M., and $n=9$ animals per group. One-way ANOVA was used to assess the statistical significance of the group differences (** $p<0.01$ in relation to the immediately preceding stage; $\Delta p<0.01$, BFD versus PW7).

PW5 ($p<0.01$, PW3 versus PW5) (Figure 4B). After PW5, the mean relative level of PTP σ increased until adulthood ($p<0.05$, PW7 versus PW9), when it reached the same level observed at the beginning of the critical period ($p>0.05$, PW9 versus PW3) (Figure 4B). However, BFD could decrease PTP σ protein expression after the critical period ($p<0.01$, BFD versus PW7/PW9 (Figure 4B).

Changes in the Number of PV/WFA/PTP σ -Labeled VC Cells During the Critical Period and After BFD

Analysis of the PV/WFA/PTP σ labeling demonstrated the presence of triple-labeled cells in the VC (Figure 5). Because the density of WFA labeled somata

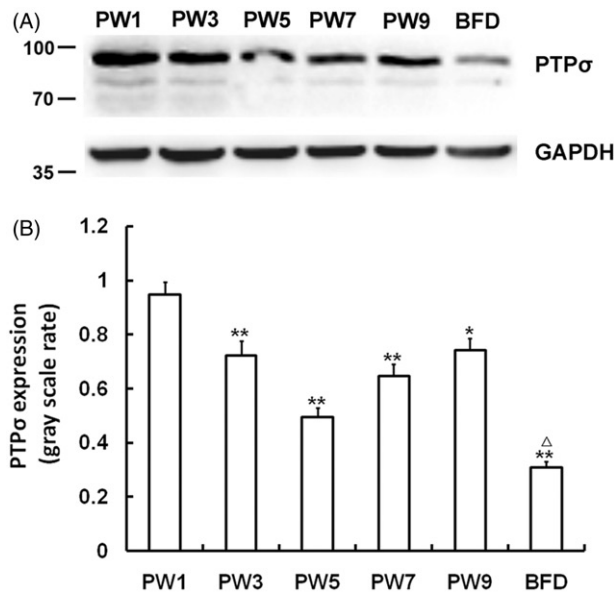


FIGURE 4 Representative western blots showing PTP σ in the rat visual cortex during development and after BFD. (A): Western blot of visual cortex taken at different groups, probed for PTP σ or GAPDH. (B): Quantification of western blot results. PTP σ levels were normalized to GAPDH. Values are expressed as the mean \pm S.E.M., $n=9$ animals per group. One-way ANOVA was used to assess the statistical significance of the group differences (** p < 0.01; * p < 0.05 in relation to the immediately preceding stage; Δp < 0.01, BFD versus PW7).

(PNNs) was generally higher in layer IV than in the other layers (about twice the density) and because layer IV is the major termination site for geniculate axons,^{3,22} we analyzed the developmental changes in the number of triple-labeled cells in this layer. At PW3, although the number of PV neurons was at its highest, the percentage of PV/WFA/PTP σ positive cells in relation to total PV population was the lowest ($31.69 \pm 5.43\%$; p < 0.01) (Figure 6B), due to the lowest density of PNNs. The number of PV/WFA/PTP σ positive cells was highest at PW5 (p < 0.01) and then declined at PW7 (Figure 6A), most likely due to the decrease in PV neurons. A small but significant increase was observed at PW9 (p < 0.01, PW7 versus PW9), with the highest ratio of PV/WFA/PTP σ positive cells ($82.20 \pm 4.07\%$; p < 0.01), which is consistent with the significant increase in PTP σ - and WFA-positive cells at PW9 (Figure 6). However, after BFD, the number of triple-labeled cells decreased significantly (p < 0.05, BFD versus PW7; p < 0.01, BFD versus PW9), and the proportion of triple-labeled PV neurons also decreased (p < 0.01, BFD versus PW7/PW9) (Figure 6).

DISCUSSION

Our experiments show that the number of PV neurons wrapped by PNNs increased markedly between PW3 and PW5 and then stayed at a relatively high level

until adulthood. The increase in the ratio of WFA/PV positive cells to PV neurons was also particularly prominent in the first half of the critical period and reached the highest level at adulthood. BFD decreased the expression of PNNs and the percentage of PV neurons with PNNs. However, the CSPG receptor PTP σ followed a different profile of expression during postnatal VC development. The expression of PTP σ declined after PW1 and stayed at its lowest level during the critical period. Interestingly, after the critical period (PW9), the expression of PTP σ recovered to the same level observed at the start of the critical period (PW3). BFD decreased the expression of PTP σ in the VC after the critical period. In layer IV, the percentage of PV/WFA/PTP σ positive cells in relation to the total PV population increased during development was highest at adulthood and could also be decreased by BFD.

CSPGs are abundant in the extracellular matrix of the brain, and they inhibit axonal growth during development and regeneration following spinal cord injury *in vivo*.¹⁵ WFA binds indirectly or directly to chondroitin sulfate, and its reactivity has become a standard method of identifying chondroitin sulfate-containing subsets of neurons in the central nervous system that are surrounded by lattice-like cell coatings forming the PNNs.^{23,24} It has previously been shown that the amount of WFA increases in all cortical layers during development and reaches adult levels at P70, but WFA is most prevalent in layer IV.³ Our results also showed that the density of WFA-positive cells increased with age until at least PW9. CSPGs are involved in ocular dominance plasticity. After CSPG degradation with chondroitinase ABC in adult rats, monocular deprivation caused an ocular dominance shift towards the non-deprived eye.³ Environmental enrichment also decreased the density of PNNs in all layers along with the restoration of visual plasticity in adult rats.²⁵ Moreover, our data showed that BFD at the end of the critical period could decrease the densities of PNNs in layers II–III and layer IV. It has been reported that BFD modulates the plasticity of the juvenile and adult VC by modulating the NMDA receptor signaling.^{4,19} Our results suggested that the changes in PNN density in the VC might be involved in the recovery of plasticity after BFD.

In the VC, PV-immunoreactive neurons first appear in the middle layers and later cover the whole extent of layers II–VI and are more prevalent in the middle and lower cortical layers.²⁶ The number of PV neurons in the VC first peaks at around PW3 (the start of the critical period), and then rapidly decreases to the adult level during the middle of the critical period,^{26,27} in agreement with the present data. Moreover, our results showed that BFD at the end of the critical period could not change the number of PV neurons.

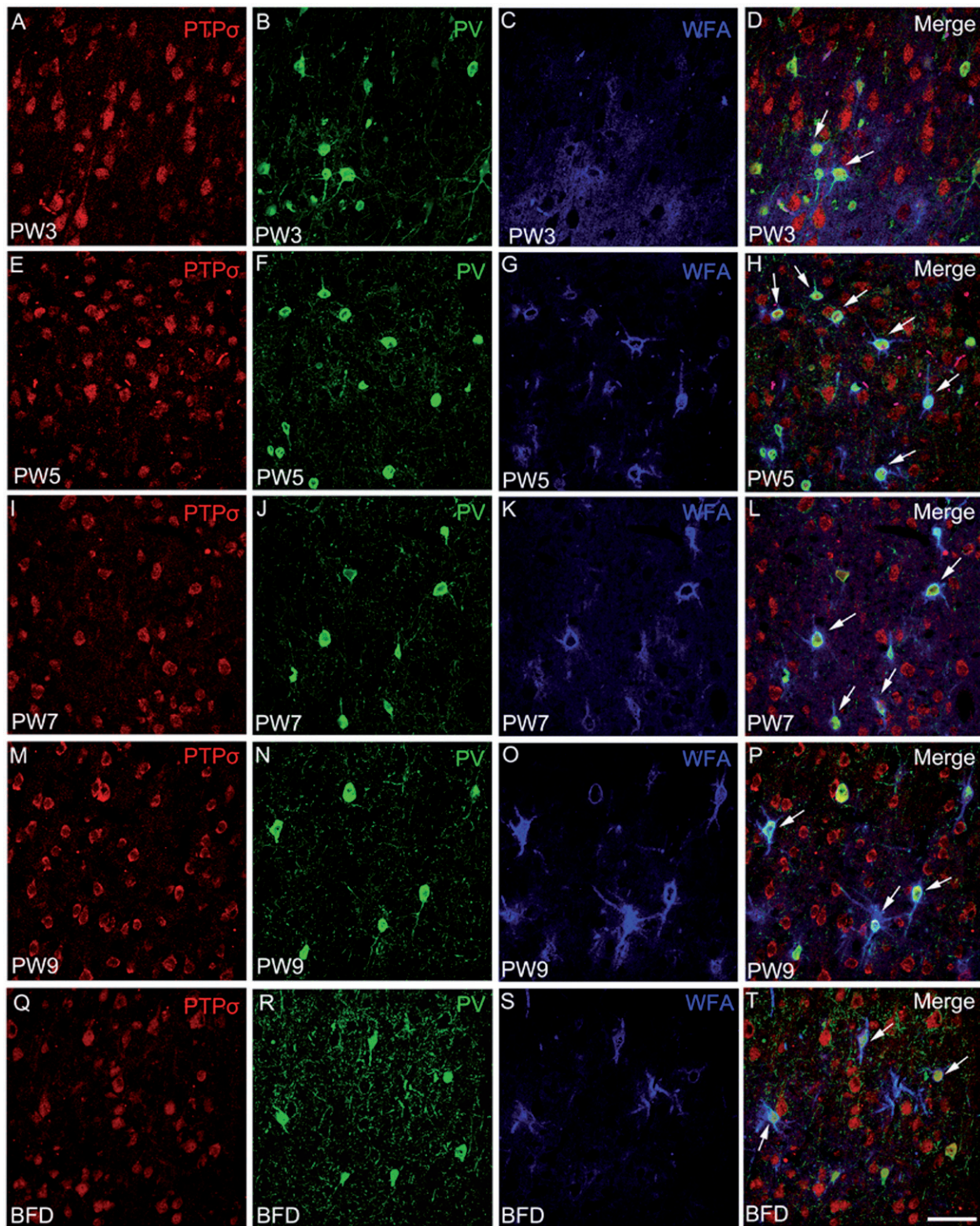


FIGURE 5 Triple immunohistochemical labeling of PTP σ (red), PV (green), WFA (blue), and the overlay of the three markers (pseudo-color white, merge) in layer IV of the primary visual cortex from different groups, PW3 (A–D), PW5 (E–H), PW7 (I–L), PW9 (M–P), and BFD (Q–T). White arrows indicate PV/WFA/PTP σ triple-labeled neurons. Scale bar = 50 μ m.

Intriguingly, morphological evidence has shown that most of the PNNs are around PV neurons^{3,24,28} and ensheathe the soma and the proximal parts of dendrites (Figure 5). However, we noticed that the

ratio of WFA/PV positive cells to WFA-positive cells decreased with age, indicating that approximately 30% of PNNs gradually surrounded PV-negative neurons during the critical period. Our results also

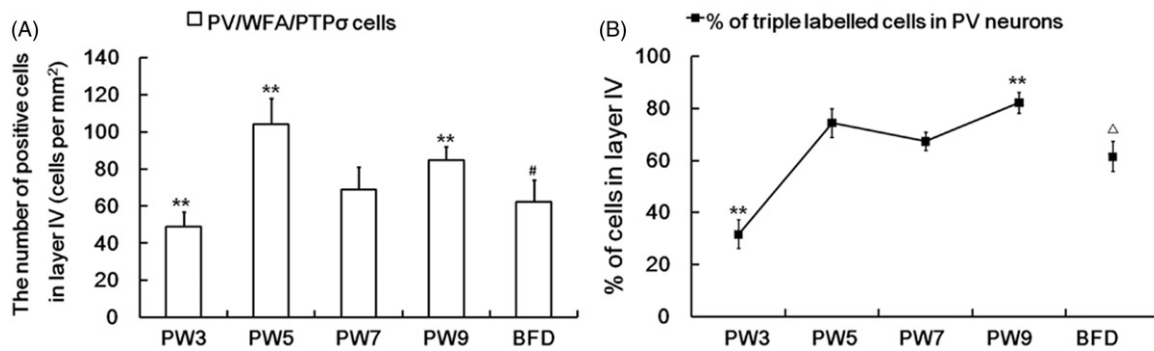


FIGURE 6 Quantitative analysis of PV/WFA/PTP σ triple-labeled neurons in layer IV of the rat primary visual cortex from different groups. Values are expressed as the mean \pm S.E.M., $n=9$ animals per age. Mann–Whitney U -test was used to assess the statistical significance of the group differences. (A): ** p < 0.01, PW3/PW5/PW9 versus other group; # p < 0.05, BFD versus PW7. (B): ** p < 0.01, PW3/PW9 versus other group; Δ p < 0.01, BFD versus PW7.

showed the developmental profile of the number of WFA/PV neurons, which increased markedly between PW3 and PW5 and then stayed at a relatively high level until adulthood. The percentage of PV neurons wrapped by PNNs also increased and reached the highest level at adulthood (over 75%), indicating that PNNs may play an important role in the maturation of PV neurons during the critical period. BFD could decrease the ratio for PV neurons, as the number of PV neurons stayed constant, suggesting that the expression of PNNs surrounding PV neurons could be experience-dependent. PNNs may serve as rapid local buffers of excess cation changes in the extracellular space²⁹ and subserve fast inhibitory interneuronal actions in visual information processing.³⁰ However, the underlying mechanism by which CSPGs modulate the neuronal plasticity of PV-neurons remains largely elusive.

Similar to chondroitinase ABC treatment, PTP σ gene knockout promotes neurite outgrowth in the presence of CSPG *in vitro* and enhances axonal growth into CSPG-rich scar tissue following spinal cord injuries *in vivo*.^{8,31} Although the intensity of PTP σ expression overall gradually decreases during embryonic development,⁹ it is maintained at relatively high levels in the neurons of the postnatal and adult nervous system.^{9,16,32} Our data show that PTP σ expression detected by PCR or western blots was highest in the VC at PW1, which was in agreement with the widely accepted expression pattern of PTP σ revealed by *in situ* hybridization analysis during the development of the cortex.^{16,33} In our results, PTP σ appears even before the beginning of the critical period (PW3), which is prior to the appearance of CSPGs and PV neurons during VC development. This finding suggests that PTP σ may be involved directly in brain development in addition to its role as an inhibitory receptor and that it may also participate in pituitary cytodifferentiation and hormone production.³⁴ Interestingly, we found that PTP σ expression stayed at a relatively low level during the critical

period of the VC, possibly facilitating the formation of synaptic connections by attenuating the inhibitory effect of CSPGs. Meanwhile, BFD could decrease the mRNA and protein levels of PTP σ and the numbers of PTP σ -positive cells in all layers of the VC, indicating that the expression of PTP σ could be regulated by visual experience.

It has been documented that the majority of PTP σ mRNA is expressed in neurons, especially the 5.7 kb transcript.¹⁶ Our immunohistochemistry results also showed that most of the PTP σ -positive cells in adult VC were neurons. Interestingly, PV neurons wrapped by PNNs also expressed the CSPG receptor PTP σ , which hinted at a connection between PTP σ and PV neurons. In our results, after entering the critical period, more CSPGs condensed around PV cells, thus playing a crucial role in the increased proportion of layer IV PV neurons that were also positive for WFA and PTP σ . We also found that this process could be reversed by BFD even after the end of the critical period. It has been observed that the maturation of PV cells over the course of the critical period is regulated by brain-derived neurotrophic factor (BDNF).⁶ Recently, some studies have shown that CSPGs target and dephosphorylate tropomyosin-related kinase B (TrkB), the receptor for BDNF, via PTP σ and that they suppress spine formation induced by BDNF in cortical neurons.³⁵ It is known that the majority of PV neurons in rat visual cortex express TrkB, but most other visual cortex interneurons do not.³⁶ Combining this literature with our results, we deduced that CSPGs may curb the experience-dependent formation of new synapses on PV neurons. Through TrkB, BDNF also acutely depresses excitatory synaptic transmission to GABAergic neurons whose inhibitory output to pyramidal neurons is thereby depressed.³⁷ GABA α 1 subunits on pyramidal neurons, which form the circuits that drive cortical plasticity, are localized in receptors that specifically receive PV-positive afferents.^{5,38} As PTP σ regulates excitatory synapse formation in a

bidirectional manner,^{33,39} future research should assess whether the opposing effect of CSPGs against BDNF via PTP σ could strengthen the excitatory synaptic transmission to PV neurons, thus potentiating inhibitory transmission to pyramidal neurons.

ACKNOWLEDGEMENTS

The authors thank Yaochen Li, Yuxiao Zeng, Chuanhuang Weng, Jianrong He for excellent technical support; they also thank technician Wei Sun (Central Laboratory, Third Military Medical University, Chongqing, China) for her assistance in laser scanning confocal microscopy. We thank Dr T. FitzGibbon for comments on earlier drafts of the manuscript.

DECLARATION OF INTEREST

This study was supported by the National Basic Research Program of China (No. 2013CB967002) and National Natural Sciences Foundation of China (81070749).

There are no commercial relationships either in the form of financial support or as personal financial interests.

REFERENCES

- Berardi N, Pizzorusso T, Maffei L. Extracellular matrix and visual cortical plasticity: freeing the synapse. *Neuron* 2004; 44:905–908.
- He HY, Hodos W, Quinlan EM. Visual deprivation reactivates rapid ocular dominance plasticity in adult visual cortex. *J Neurosci* 2006;26:2951–2955.
- Pizzorusso T, Medini P, Berardi N, Chierzi S, Fawcett JW, Maffei L. Reactivation of ocular dominance plasticity in the adult visual cortex. *Science* 2002;298:1248–1251.
- Sato M, Stryker MP. Distinctive features of adult ocular dominance plasticity. *J Neurosci* 2008;28:10278–10286.
- Fagiolini M, Fritschy JM, Löw K, Möhler H, Rudolph U, Hensch TK. Specific GABA A circuits for visual cortical plasticity. *Science* 2004;303:1681–1683.
- Huang ZJ, Kirkwood A, Pizzorusso T, Porciatti V, Morales B, Bear MF, et al. BDNF regulates the maturation of inhibition and the critical period of plasticity in mouse visual cortex. *Cell* 1999;98:739–755.
- Grabert J, Wahle P. Visual experience regulates Kv3.1b and Kv3.2 expression in developing rat visual cortex. *Neuroscience* 2009;158:654–664.
- Shen Y, Tenney AP, Busch SA, Horn KP, Cuascut FX, Liu K, et al. PTP σ is a receptor for chondroitin sulfate proteoglycan, an inhibitor of neural regeneration. *Science* 2009;326:592–596.
- Yan H, Grossman A, Wang H, D'Eustachio P, Mossie K, Musacchio JM, et al. A novel receptor tyrosine phosphatase-sigma that is highly expressed in the nervous system. *J Biol Chem* 1993;268:24880–24886.
- Stepanek L, Stoker AW, Stoeckli E, Bixby JL. Receptor tyrosine phosphatases guide vertebrate motor axons during development. *J Neurosci* 2005;25:3813–3823.
- Uetani N, Chagnon MJ, Kennedy TE, Iwakura Y, Tremblay ML. Mammalian motoneuron axon targeting requires receptor protein tyrosine phosphatases sigma and delta. *J Neurosci* 2006;26:5872–5880.
- Johnson KG, McKinnell IW, Stoker AW, Holt CE. Receptor protein tyrosine phosphatases regulate retinal ganglion cell axon outgrowth in the developing *Xenopus* visual system. *J Neurobiol* 2001;49:99–117.
- Ledig MM, Haj F, Bixby JL, Stoker AW, Mueller BK. The receptor tyrosine phosphatase CRYPalphalpha promotes intraretinal axon growth. *J Cell Biol* 1999;147:375–388.
- Johnson KG, Van Vactor D. Receptor protein tyrosine phosphatases in nervous system development. *Physiol Rev* 2003;83:1–24.
- Duan Y, Giger RJ. A new role for RPTP σ in spinal cord injury: signaling chondroitin sulfate proteoglycan inhibition. *Sci Signal* 2010;3:pe6.
- Wang H, Yan H, Canoll PD, Silvennoinen O, Schlessinger J, Musacchio JM. Expression of receptor protein tyrosine phosphatase-sigma (RPTP-sigma) in the nervous system of the developing and adult rat. *J Neurosci Res* 1995;41:297–310.
- Sapieha PS, Duplan L, Uetani N, Joly S, Tremblay ML, Kennedy TE, et al. Receptor protein tyrosine phosphatase sigma inhibits axon regrowth in the adult injured CNS. *Mol Cell Neurosci* 2005;28:625–635.
- Zheng S, Yin ZQ, Zeng YX. Developmental profile of tissue plasminogen activator in postnatal Long Evans rat visual cortex. *Mol Vis* 2008;14:975–982.
- Qin W, Yin ZQ, Wang S, Zhao Y. Effects of binocular form deprivation on the excitatory post-synaptic currents mediated by N-methyl-D-aspartate receptors in rat visual cortex. *Clin Experiment Ophthalmol* 2004;32:289–293.
- Li Z, Gao C, Huang H, Sun W, Yi H, Fan X, et al. Neurotransmitter phenotype differentiation and synapse formation of neural precursors engrafting in amyloid- β (1–40) injured rat hippocampus. *J Alzheimers Dis* 2010;21:1233–1247.
- Tropea D, Capsoni S, Tongiorgi E, Giannotta S, Cattaneo A, Domenici L. Mismatch between BDNF mRNA and protein expression in the developing visual cortex: the role of visual experience. *Eur J Neurosci* 2001;13:709–721.
- Yin ZQ, Crewther SG, Wang C, Crewther DP. Pre- and post-critical period induced reduction of Cat-301 immunoreactivity in the lateral geniculate nucleus and visual cortex of cats Y-blocked as adults or made strabismic as kittens. *Mol Vis* 2006;12:858–866.
- Ajmo JM, Eakin AK, Hamel MG, Gottschall PE. Discordant localization of WFA reactivity and brevican/ADAMTS-derived fragment in rodent brain. *BMC Neurosci* 2008;9:14.
- Härtig W, Brauer K, Bigl V, Brückner G. Chondroitin sulfate proteoglycan-immunoreactivity of lectin-labeled perineuronal nets around parvalbumin-containing neurons. *Brain Res* 1994;635:307–311.
- Sale A, Maya Vetencourt JF, Medini P, Cenni MC, Baroncelli L, De Pasquale R, et al. Environmental enrichment in adulthood promotes amblyopia recovery through a reduction of intracortical inhibition. *Nat Neurosci* 2007;10:679–681.
- Hof PR, Glezer II, Condé F, Flagg RA, Rubin MB, Nimchinsky EA, et al. Cellular distribution of the calcium-binding proteins parvalbumin, calbindin, and calretinin in the neocortex of mammals: phylogenetic and developmental patterns. *J Chem Neuroanat* 1999;16:77–116.
- Hada Y, Yamada Y, Imamura K, Mataga N, Watanabe Y, Yamamoto M. Effects of monocular enucleation on

- parvalbumin in rat visual system during postnatal development. *Invest Ophthalmol Vis Sci* 1999;40:2535–2545.
28. Wegner F, Härtig W, Bringmann A, Grosche J, Wohlfarth K, Zuschritter W, et al. Diffuse perineuronal nets and modified pyramidal cells immunoreactive for glutamate and the GABA(A) receptor alpha1 subunit form a unique entity in rat cerebral cortex. *Exp Neurol* 2003;184:705–714.
 29. Härtig W, Derouiche A, Welt K, Brauer K, Grosche J, Mäder M, et al. Cortical neurons immunoreactive for the potassium channel Kv3.1b subunit are predominantly surrounded by perineuronal nets presumed as a buffering system for cations. *Brain Res* 1999;842:15–29.
 30. Seeger G, Lüth HJ, Winkelmann E, Brauer K. Distribution patterns of *Wisteria floribunda* agglutinin binding sites and parvalbumin-immunoreactive neurons in the human visual cortex: a double-labelling study. *J Hirnforsch* 1996;37:351–366.
 31. Fry EJ, Chagnon MJ, López-Vales R, Tremblay ML, David S. Corticospinal tract regeneration after spinal cord injury in receptor protein tyrosine phosphatase sigma deficient mice. *Glia* 2010;58:423–433.
 32. Schaapveld RQ, van den Maagdenberg AM, Schepens JT, Weghuis DO, Geurts van Kessel A, Wieringa B, et al. The mouse gene Ptprf encoding the leukocyte common antigen-related molecule LAR: cloning, characterization, and chromosomal localization. *Genomics* 1995;27:124–130.
 33. Kwon SK, Woo J, Kim SY, Kim H, Kim E. Trans-synaptic adhesions between netrin-G ligand-3 (NGL-3) and receptor tyrosine phosphatases LAR, protein-tyrosine phosphatase delta (PTPdelta), and PTPsigma via specific domains regulate excitatory synapse formation. *J Biol Chem* 2010;285:13966–13978.
 34. Batt J, Asa S, Fladd C, Rotin D. Pituitary, pancreatic and gut neuroendocrine defects in protein tyrosine phosphatase-sigma-deficient mice. *Mol Endocrinol* 2002;16:155–169.
 35. Kurihara D, Yamashita T. Chondroitin sulfate proteoglycans down-regulate spine formation in cortical neurons by targeting tropomyosin-related kinase B (TrkB) protein. *J Biol Chem* 2012;287:13822–13828.
 36. Gorba T, Wahle P. Expression of TrkB and TrkC but not BDNF mRNA in neurochemically identified interneurons in rat visual cortex in vivo and in organotypic cultures. *Eur J Neurosci* 1999;11:1179–1190.
 37. Jiang B, Kitamura A, Yasuda H, Sohya K, Maruyama A, Yanagawa Y, et al. Brain-derived neurotrophic factor acutely depresses excitatory synaptic transmission to GABAergic neurons in visual cortical slices. *Eur J Neurosci* 2004;20:709–718.
 38. Klausberger T, Roberts JD, Somogyi P. Cell type- and input-specific differences in the number and subtypes of synaptic GABA(A) receptors in the hippocampus. *J Neurosci* 2002;22:2513–2521.
 39. Takahashi H, Arstikaitis P, Prasad T, Bartlett TE, Wang YT, Murphy TH, et al. Postsynaptic TrkC and presynaptic PTP σ function as a bidirectional excitatory synaptic organizing complex. *Neuron* 2011;69:287–303.